46th EPS Conference on Contr. Fusion and Plasma Phys., Milan, 8-12 July 2019

Progress on understanding ELM destabilization via thermoelectric currents

M. Knolker[1], T. Evans[1], R. Moyer[2], C. Paz-Soldan[1], A. Wingen[3], A. Bortolon[4], F. Laggner[4], H. Zohm[5]

[1] *General Atomics, San Diego, USA*

[2] *University of California at San Diego, San Diego, USA*

[3] *Oak Ridge National Laboratory Oak Ridge, USA*

[4] *Princeton Plasma Physics Laboratory, Princeton, USA*

[5] *Max Planck Institut für Plasmaphysik, Munich, Germany*

Introduction

Type I-ELM energy impulses and heat loads are of great concern for ITER and future power plants as they can lead to divertor erosion and melting[1]. Hence, the investigation of the explosive (non-linear) ELM phase and its dynamics is indispensable for progress on ELM control and understanding. Recently, an additional driver of explosive growth in the nonlinear ELM phase has been identified on DIII-D in the form of stochasticity enhancing non-axisymmetric thermoelectric currents that flow through helical flux tubes in the confined plasma[2]. These currents are measured with an array of shunted divertor tiles and undergo rapid oscillations in a time interval amounting up to 0.1 ms before a significant increase in divertor heat flux occurs. Extrapolating this current results in a peak of 5-20 kA flowing in a concentric circle near the strike point in agreement with similar measurements from other machines[3]. Toroidal analysis of these currents is consistent with a low n mode composition which will affect stability and transport in the nonlinear phase[4]. An ELM current model (ECM) has been developed based on the thermoelectric origin of the tile currents and is found consistent with the current measurements[2,5]. Here, the ECM is briefly introduced and progress on experimental validation is reported.

Overview of the ELM current model and validation

The ECM proposes the following ELM process:

- After exceeding the peeling-ballooning stability threshold, particle and energy loss from the pedestal cause electron heat pulses that locally increase the divertor plasma temperature near the surface of the target plate on a parallel heat conduction timescale

- Thermoelectric currents flow from the hot divertor plasma to respective colder regions on the cold divertor side (in forward B_T, the low field side is the hot divertor side). Employing the advanced field line tracing code MAFOT[6] and resistance calculations using thermoelectric current models suggest partial current flow through flux tubes in the confined plasma inside of the separatrix (produced by error fields and the ballooning modes) with the ion saturation current as upper limit.
- Through a self-amplifying mechanism, more and larger flux tubes are produced due to currents in the flux tubes which facilitates access to deeper layers of the pedestal causing additional heat and particle transport as edge resonant magnetic islands overlap producing a widening layer of stochasticity
- The drive for the thermoelectric current ceases through nonlinear saturation mechanisms and the pedestal recovery sets in

A validation of the ECM helical current path through the plasma has been provided through analysis of Double Null plasmas, where the increase of ELM currents is measured simultaneously on high and low field side[2]. Pure current flow in the SOL cannot explain this instant rise on the high field side as it would take finite time for the perturbation to spread there; hence currents are flowing through the confined plasma.

Progress and experimental findings

The ECM prompts the physics question of how strong the impact of the currents on the ELM transport is, i.e. are large thermoelectric currents required for large ELM sizes? In a first approach, type- I ELMs in DIII-D in inner wall limited plasmas (IWL) were investigated. In contrast to diverted plasmas, IWL plasmas do not have an axisymmetric X-point nor strike points and hence there usually is no connection of field lines through the confined plasma to balance divertor temperature differences (Figure 1). An exception could be reduced currents through flux tube structures right on the plasma wall interface. A typical discharge with B_T=2.0 T, I_P=1.3 MA and a stored energy of W_{MHD}=0.6 MJ and P_{NBI}=7.5 MW is selected from a study of n=1 islands in IWL plasmas[7]. The ELM frequency amounts to 70 Hz with a most unstable mode number of n=20 as shown by ELITE[8]

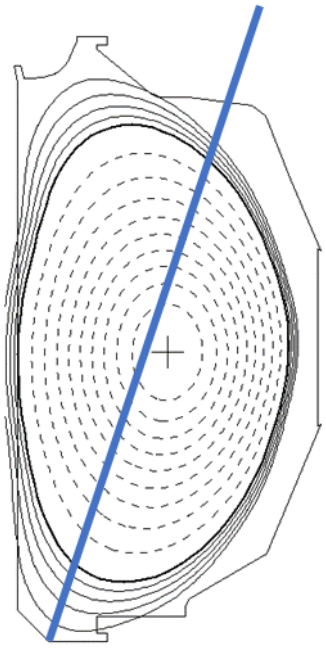

Figure 1 Equilibrium of inner wall limited H-mode discharge with Dα filterscope line of view

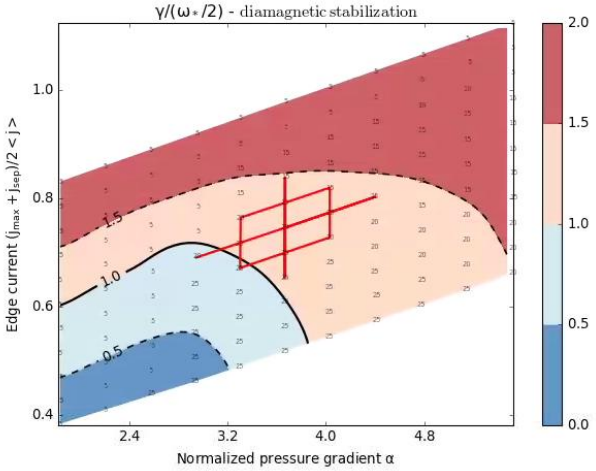

Figure 2 Linear Stability analysis with ELITE on 80-99 % ELM cycle of discharge 154528 confirms the type I ELM nature of the IWL plasma with n=20 as most unstable mode number

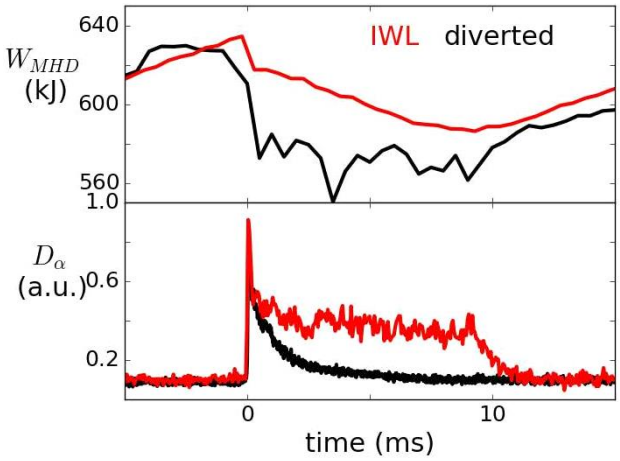

Figure 3 Comparison of IWL (154528) and diverted plasma ELM (153527): a) stored plasma energy b) filterscope as indicated in figure 1

analysis (figure 2). Based on the results of previous ELM studies[9], plasmas with the same energy and similar density were chosen yielding comparable relative ELM sizes of up to 10%. As shown in figure 3, one can see that the ELMs in this plasma are different than ELMs from similar (yet diverted) plasmas. The energy loss occurs over a much longer time period (with a slower loss per unit time) than in the diverted case. This is based on the measurement of stored energy by fast magnetic probes and the Dα radiation. These predictions are consistent with the ECM, since the non-existence of strong thermoelectric currents leads to a lack of explosive growth in the IWL case and a much slower development of the instability.

Another example of the effect of the currents on ELMs can be studied by revisiting a previous DIII-D divertor configuration with a biased ring[10]. The ring was part of the outer divertor and insulated against the vessel. In a dedicated study the impact of ring bias on ELMs was investigated. In these discharges the outer strike point was positioned on the ring with B_T=2.1T, I_P= 0.8 MA and P_{NBI} = 5-8 MW. As shown in figure 4, the application of the ring bias in this configuration leads to a large current flow of 3 kA and to a change of ELM nature, indicated by the decrease of Dα filterscope signals near the inner strike point (also seen in RMP ELM suppression experiments). This is qualitatively consistent with the idea that biasing the divertor and

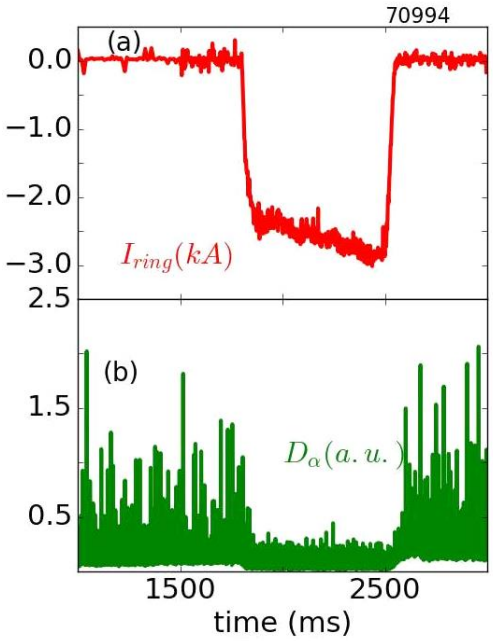

Figure 4 Biasing effects on ELMs a) Ring current b) Dα filterscope indicating changes in ELM deposition pattern

hence changing the ELM currents could affect the ELM size. Unfortunately, neither fast stored energy or IR signals nor measurements from the outer strike point are available for these discharges, so that the reduction of ELM size cannot be quantified.

Conclusions und future work

The measurements and findings presented in this work deliver further confirmation of the ELM current model and encourage implementing tile currents into nonlinear ELM simulations. The stochasticity increasing current mechanism could provide the explosive nonlinear growth that has been sought in computational ELM simulations in order to provide the measured fast heat flux rise in the divertor[11,12]. Moreover, experimental measurements on DIII-D encourage further divertor biasing experiments on mid-size tokamaks to explore and quantify the potential of ELM mitigation on future fusion power plants.

This material is based upon work supported by the U.S. Department of Energy, Office of Science, Office of Fusion Energy Sciences, using the DIII-D National Fusion Facility, a DOE Office of Science user facility, under Awards DE-AC05-00OR22725, DE-AC02-09CH11466, and DE-FC02-04ER54698. This research was supported by the General Atomics Postgraduate Research Participation Program administered by ORAU.

References

[1] A.W. Leonard, Phys. Plasmas **21** (2014).
[2] M. Knolker, Nucl. Fusion submitted, (2019).
[3] A. Kallenbach et al, Nucl. Fusion **48** (2008).
[4] M. Knolker et al, Nucl. Mater. Energy **18**, 222 (2019).
[5] T.E. Evans et al, J. Nucl. Mater. 390–391, **789** (2009).
[6] A. Wingen et al, Phys. Rev. Lett. **104**, (2010).
[7] T.E. Evans, Plasma Phys. Control. Fusion **57** (2015).
[8] P.B. Snyder et al, Phys. Plasmas **9** (2002), pp. 2037–2043.
[9] M. Knolker et al, Nucl. Fusion **58**, 096023 (2018).
[10] M.J. Schaffer and B.J. Leikind, Nucl. Fusion **31**, 1750 (1991).
[11] L.E. Sugiyama and H.R. Strauss, Phys. Plasmas **17**, (2010).
[12] S. Pamela et al, Plasma Phys. Control. Fusion **58**, (2015).